Assessing and characterizing oilseed rape freezing injury based on MODIS and MERIS data

She Bao[1], Huang Jingfeng[1,2,3*], Zhang Dongyan[4], Huang Linsheng[4]

(1. *Institute of Agricultural Remote Sensing and Information Technology Application, Zhejiang University, Hangzhou 310058, China*;
2. *Key Laboratory of Agricultural Remote Sensing and Information System, Zhejiang Province, Hangzhou 310058, China*;
3. *Key Laboratory of Environment Remediation and Ecological Health, Ministry of Education, Hangzhou 310058, China*;
4. *Anhui Engineering Laboratory of Agro-ecological Big Data, Anhui University, Hefei 230601, China*)

Abstract: The oilseed rape growing in the lower reaches of Yangtze River in China belongs to winter varieties and suffers the risk of freezing injury. In this research, a typical freezing injury event occurred in Anhui Province was taken as a case study, the freezing damage degree of oilseed rape was assessed, and its development characteristics based on the vegetation metrics derived from MODIS and MERIS data were investigated. The oilseed rape was mapped according to the decline of greenness from bud stage to full-bloom period, with the phenological phases identified adopting time-series analyses. NDVI was more sensitive to freezing injury compared with other commonly used vegetation indices (VIs) calculated using MODIS bands, e.g., EVI, GNDVI and SAVI. The freezing damage degree employing the difference between post-freeze growth and the baseline level in adjacent damage-free growing seasons was determined. The remote sensing-derived damage levels were supported by their correlation with the cold accumulated temperatures at the county level. The performance of several remote sensing indicators of plant biophysical and biochemical parameters was also investigated, i.e., the photosynthetic rate, canopy water status, canopy chlorophyll content, leaf area index (LAI) and the red edge position (REP), in response to the advance of the freezing damage. It was found that the photosynthetic rate indicator—Photochemical Reflectance Index (PRI) responded strongly to freezing stress. Freezing injury caused canopy water loss, which could be detected though the magnitude was not very large. MERIS-LAI showed a slow and lagging response to low temperature and restored rapidly in the recovery phase; additionally, REP and the indicator of canopy chlorophyll content—MERIS Terrestrial Chlorophyll Index (MTCI), did not appear to be influenced by freezing injury. It was concluded that the physiological functions, canopy structure, and organic content metrics showed a descending order of vulnerabilities to freezing injury.

Keywords: *Brassica napus*, oilseed rape, freezing injury, crop monitoring, MODIS, MERIS
DOI: 10.3965/j.ijabe.20171003.2721

Citation: She B, Huang J F, Zhang D Y, Huang L S. Assessing and characterizing oilseed rape freezing injury based on MODIS and MERIS data. Int J Agric & Biol Eng, 2017; 10(3): 143–157.

1 Introduction

Oilseed rape (*Brassica napus* L.) is a widely cultivated oil crop, and China has the second largest sown area in the world. About 90% of the oilseed rapes in China are winter varieties which concentrate mainly in the middle and lower reaches of Yangtze River. The winter oilseed rapes are generally sown in autumn and mature in spring or early summer in the next year, and are usually rotated with paddy rice or cotton.

The wintering period is essential to the reproductive growth of oilseed rape (hereinafter refers specially to winter varieties), during which it accomplishes the vernalization and flower bud can thus form in the future. However, the special geographical location of the lower reaches of Yangtze River (especially in the transition

Receive date: 2016-07-20 **Accepted date:** 2016-12-08
Biographies: She Bao, PhD candidate, research interests: crop damage detection and assessment, Email: shebao518@163.com; **Zhang Dongyan**, PhD, Associate Professor, research interest: crop damage detection, Email: hello-lion@hotmail.com; **Huang Linsheng**, PhD, Associate Professor, research interest: crop damage detection, Email: linsheng0808@163.com.
***Corresponding author: Huang Jingfeng**, PhD, Professor, research interests: agricultural remote sensing and information technology application. No. 866 Yuhangtang Road, Hangzhou 310058. Tel/Fax: +86-571-8898-2830; Email: hjf@zju.edu.cn.

zone between the north and south China in meteorology) exposes the oilseed rape to freezing weather threats, fortunately not very frequent. The freezing damage has long been one of the major causes contributing to the production loss of oilseed rape due to its relatively weak cold-resistance capacity. It is noted that as the climate warming continues, the extended phenology before the wintering period of oilseed rape might lead it more vulnerable to freezing injury[1], partially due to the excess premature development and inadequate cold-acclimation[2].

The influence of excessive low temperature on the growth and reproduction of oilseed rape has already been studied. For example, Lardon and Triboi-Blondel[3] found that freezing stress resulted in shriveled ovule and inhibited seed filling, and the germination potential of stressed seeds was closely related to the time interval between fertilization and freezing treatment. Rapacz[4] observed that the level of growth activity determined re-acclimation ability, when fully cold-acclimated oilseed rape seedlings were subjected to deacclimation in higher temperature and then transferred back to the cold-acclimating conditions, their re-acclimation ability was limited if elongation growth had begun during deacclimation. Cold treatment to oilseed rape from the beginning of flowering phase showed that the cold stress increased branching and lengthened the flowering period, and more pods were produced but were poorly filled[5]. By mounting a digital camera right above the oilseed rape canopy to track its vegetative development, Behrens and Diepenbrock[6] found that freezing damage led to reductions in soil coverage and the loss of small plants, leaf area index (LAI) decline started at daily mean temperatures below 5°C.

The occurrence of damage-prone freezing weather in wintertime is usually overlapped with the seedling stage of oilseed rape. To our knowledge, few studies focus on the development characteristics of oilseed rape freezing injury at the field scale. Remote sensing is an efficient approach to monitor large geographical area simultaneously at fixed time interval, and the spatial and temporal variations of surface features could be revealed and evaluated with a wealth of information provided by images. As a common practice, a variety of vegetation indices (VIs) are employed to map the degree of damage under various environmental stresses, among which, for example, the normalized difference vegetation index (NDVI) has been particularly widely used. Based on the relationship between field-measured damage intensity and SPOT-NDVI, Silleos et al.[7] assessed the frost damage of wheat occurred in Greece. Wang et al.[8] established a multiple linear regression model between plants number per unit area (denoting growth vigour) and designated several vegetation indices to monitor the freezing injury of winter wheat in China. Jurgens[9] developed the modified NDVI (mNDVI) to represent the water content of leaves and serve as a qualitative indicator of wheat frost damage. Generally, the difference between post-freeze and the baseline (pre-freeze or the annual mean) NDVIs was adopted as the freezing injury indicator, by which the magnitude of damage and its spatial pattern could be revealed[10-12]. Moreover, remote sensing-derived temperature could clearly depict the scope and extent of freezing event. For example, the AVHRR brightness temperature and surface temperature were calculated and applied to evaluate wheat frost damage in the Pampean region, Argentina, by means of linear regressions between minimum air temperature and AVHRR temperatures[13].

To our knowledge, the freezing weather process and its footprint on crop growth generally cannot last for a long time. For the oilseed rape, it is resilient to freezing stresses by nature, if not very serious. So it is a prerequisite in using remote sensing data to monitoring freezing injury that the revisit frequency of the sensor should be as short as possible to capture the essential information. The medium resolution radiometers, e.g., MODIS and MERIS, have large spatial coverage and high revisit frequency, as well as subtle spectral bands. Compared with the ordinary multispectral sensors, the medium resolution radiometers are more competent in detecting changes in vegetation state, e.g., the vegetation indices or models derived from MODIS and MERIS bands are believed to be more sensitive to certain vegetation biophysical or biochemical parameters in some scientific literature[14,15]. MODIS has 36 discrete

imaging bands, while MERIS acquires 15 programmable bands in the 390-1040 nm range of the electromagnetic spectrum, with a variable spectral bandwidth between 2.5 nm and 20 nm (10 nm on average). With high level of radiance calibration accuracy, both sensors are appropriate for quantitative assessment purposes[16,17]. Previous researches pay more attention to the pre- and post-freeze responses of vegetation, but the development features of freezing injury to crops at remote sensing level is rarely reported, especially by medium resolution radiometers like MODIS and MERIS. In this study, we took the advantages of both sensors to assess and characterize oilseed rape freezing injury from the perspective of time and space.

In this research, we aimed to study the response of oilseed rape to a typical freezing event occurred in the lower reaches of Yangtze River by using MODIS and MERIS data. We first evaluated the freezing damage severity under the premise of oilseed rape mapping, and then we traced the damage development by means of a set of combined physiologically related vegetation indices. The sensitivity of the specific VIs in their responses to freezing injury, and the change trends of certain biophysical and biochemical parameters associated with photosynthetic rate, canopy water status, green leaf area, and canopy chlorophyll content from pre- to post-freeze were also investigated.

2 Study area

We selected Anhui Province, the traditional major producing area of oilseed rape in China as the study area. Anhui locates in the lower reaches of Yangtze River, covering the geographical scope of 114°54'-119°37'E and 29°41'-34°38'N (Figure 1). The Yangtze River and Huaihe River are two major rivers flowing through the province. The northern part of Anhui is mainly plain, while the middle area is hilly, and most of the southern areas are mountainous. It has temperate semi-humid monsoon climate in the areas north of the Huaihe River, and subtropical humid monsoon climate in the rest parts. The annual average temperature is 14°C-17°C, with a precipitation of 773-1670 mm/a.

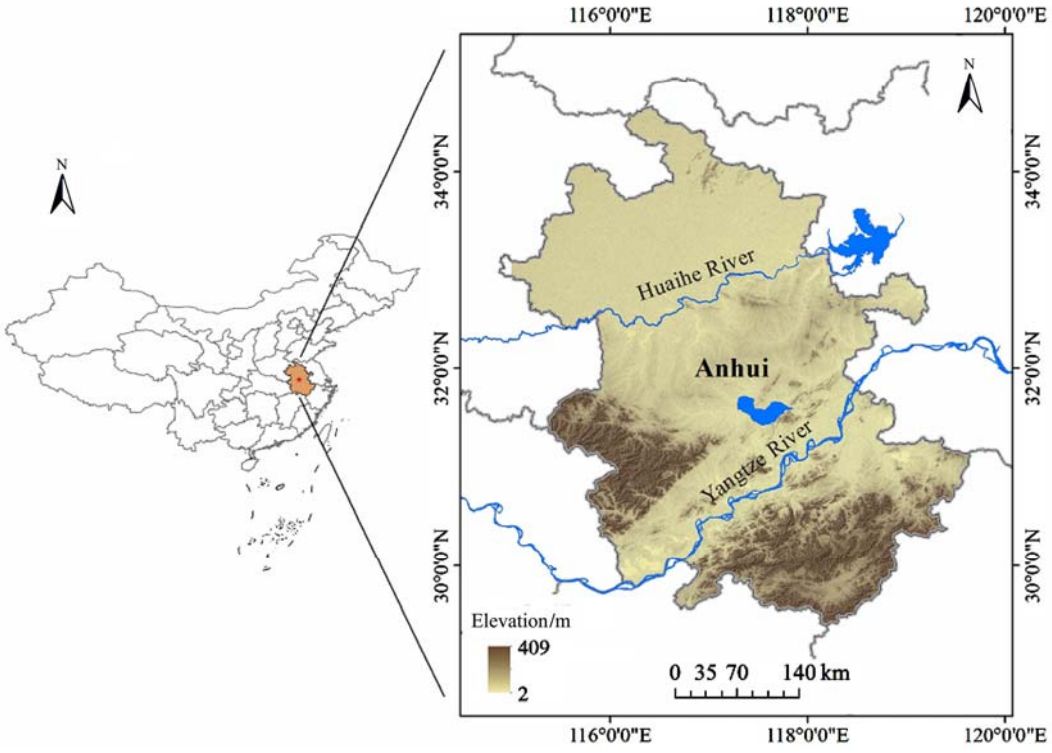

Figure 1 Map of the study area

Anhui always ranks among the top four provinces which have the largest oilseed rape cultivated area in China. All the oilseed rapes growing here are winter varieties, which are sown in late September to early October and mature in May in the next year.

The oilseed rape growing in the region between the Yangtze and Huaihe Rivers is especially vulnerable to freezing injury, because this area is situated in a climate

transition zone, where the dominating winter crop transform from winter wheat to oilseed rape gradually from north to south. In this article, we took a typical freezing event occurred in 2004 as the study case.

There were two successive freezing processes in the study area in 2004 (Figure 2), i.e., late January and early February. The lowest temperature during the first freezing process arose on January 25 (e.g., –7.7°C was observed in Hefei), the magnitude of low temperature in the second process was lesser, but considering that the oilseed rape was still in recovery from the previous freezing damage, the impact was also considerable.

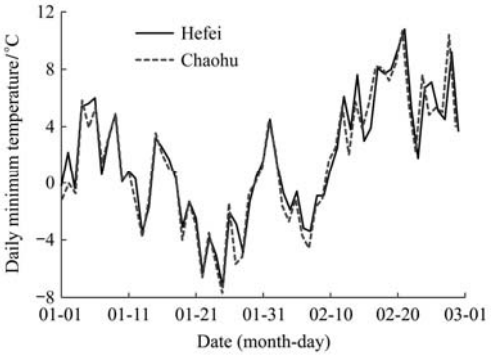

Figure 2 Daily minimum temperature observed by municipal meteorological stations in Hefei and Chaohu from January to February, 2004

Figure 3 shows the NDVI temporal profiles in 8-day composite for 2004 and adjacent 'normal' growing seasons (2001-2006 with no freezing damage, taking the average). The abrupt drop of NDVI around February 2004 clearly demonstrates the influence of the freezing injury occurred around that period.

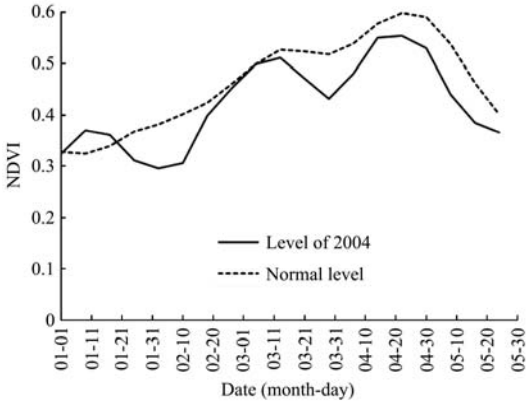

Figure 3 NDVI temporal profiles for the freezing damage-experienced and adjacent normal growing seasons. Note that each is the average of 50 different profiles extracted from the cropland in Changfeng and Feidong (two counties in Hefei), where the acreage of oilseed rape accounted for about 100% of the winter crops from statistical yearbook

3 Data and methods

3.1 Remote sensing data and preprocessing

A variety of MODIS products were used for the purpose of oilseed rape mapping, freezing injury assessment and damage-development characterizing. The MODIS surface reflectance products, 8-day composite MOD09A1 and daily gridded MOD09GA in 500 m resolution, were used to produce various vegetation indices referred in Section 3.3 (https://lpdaac.usgs.gov/). The MODIS tiles were mosaicked and reprojected to UTM coordinate system by using the MODIS Reprojection Tool (MRT), and a cloud-detection process was carried out based on the 'State QA' flag in HDF data package. Considering that not all cloudy pixels could be identified after this operation, the pixels with blue band reflectance >0.1 were also marked as cloudy[18,19].

MODIS Level 1 calibrated and geolocated radiance data were also used to calculate specific physiological indicator, i.e., the Photochemical Reflectance Index (PRI) (described later), because the desired bands were not provided by standard MODIS surface reflectance products. The MOD021KM product containing total 36 bands in 1 km resolution was adopted (https://ladsweb.nascom.nasa.gov), the pre-processing of Level-1B data included calibration, 'bow-tie' correction, geolocation, reprojection, etc. The atmospheric correction was conducted using the FLAASH module of ENVI 4.8 package. We extracted cloud cover information based on the MODIS Level 2 cloud mask product (MOD35) corresponding to each Level-1B granule, the pixels with the probability of clear ≤66% were defined as cloudy and were removed subsequently.

We also employed MERIS Level 1P reduced resolution data (http://merci-srv.eo.esa.int/merci/welcome.do), which provides 15-band calibrated radiances in 1200 m spatial resolution and 1150 km swath width. The images acquired on 7 dates, i.e., January 2, 24, 30 and February 8, 11, 15, 27 were adopted to produce specific VIs and model. The MERIS data were processed to top of canopy reflectance using the standard tools of BEAM 4.11 package. BEAM provides the corresponding modules to implement MERIS-specific

preprocessing, i.e., calibration and Smile-effect correction, cloud detection, atmospheric correction, reprojection and spatial subset.

3.2 Extraction of oilseed rape growing regions

Wheat and oilseed rape are the two main crops during wintertime in the study area, and the other vegetation in the fields could be simply ignored due to the small acreage. Wheat and oilseed rape have similar phenology throughout the growing season, and it is difficult to differentiate between them at remote sensing scales most of the time. The flowering phase is the primary signature of oilseed rape, during which the whole plant is less prominently green due to the top-down flowering, and only a fraction of leaves are remained in the bottom. The full-bloom stage arrives half a month or so after initial flowering, when the oilseed rape is in full bloom, the greenness declines correspondingly (as shown in Figure 3). In this study, we screened out oilseed rape based on NDVI variation during the time span from bud/initial flowering to full bloom stages. The identification of crop phenology was the prerequisite and foundation, we achieved this task by means of time-series analysis.

The 8-day composite surface reflectance product (MOD09A1) was employed to produce NDVI using the first two bands, and the data from the emergence of oilseed rape (DOY 289) to harvest (DOY 161 in the next year) in each growing season was adopted to generate time series. A linear interpolation procedure was implemented to replace the cloudy NDVI values with the average value of the adjacent phases[20,21], and then the NDVI time series data were smoothed by Savitzky–Golay (S-G) filter under the environment of TIMESAT 3.11[22]. A second-order polynomial method was applied, and the half-width of the smoothing window was set to 2 so as to keep the 'valley' framework of flowering segment as much as possible, and the disturbances and fluctuations caused by atmospheric variability and bi-directional effects could also be reduced simultaneously.

Considering that the start date of flowering phase varies in different areas, we adopted four schemes to identify the oilseed rape cultivated in different parts of the study area. According to the crop phenological calendar in 2001-2006 collected from the local agrometeorological stations, the beginning of main flowering period were generally identified as March 14, 22, 30 and April 7 from south to north, which were in accordance with the 8-day composite time phases. The corresponding start dates of bud/initial flowering stage were two 8-day earlier than those mentioned above, i.e., February 26, March 6, 14 and 22, respectively. The identification of oilseed rape was thus translated to the extraction of farmlands where oilseed rape were in bud stage and later full-bloom stage at different time. The bottom of the 'trough' appearing in the temporal profile represents the signature of full-bloom, and the 'peak' appearing before flowering phase describes bud stage or the onset of flowering, thereby we can identify these phenological phases based on the derivative feature of NDVI time series. For a specific time phase 't', the first and second derivative of the S-G filtered NDVI values are labelled as $f'(t)$ and $f''(t)$, the rule for filtering the oilseed rape in full bloom is designed as:

$$f'(t-1)<0, f'(t)>0 \text{ and } f''(t)>0$$

where, t is the four consecutive 8-day starting from March 14. Similarly, the rule for filtering the oilseed rape in bud stage is taken as follows:

$$f'(t-1)>0, f'(t)<0 \text{ and } f''(t)<0$$

where, t denotes the corresponding four consecutive 8-day starting from February 26. The oilseed rape pixels are supposed to be identified in both bud stage as well as flowering phase, and should meet the following requirement:

$$NDVI_{\text{bud}} > NDVI_{\text{flowering}} > 0$$

where, $NDVI_{\text{bud}}$ and $NDVI_{\text{flowering}}$ indicate the values of NDVI at any one set of the four time-phase combinations, e.g., February 26 and March 14, and so on. The union of the screened out oilseed rape fields with different flowering time was regarded as its distribution in the whole province.

In order to further improve the reliability of the extraction results, a supplementary rule was also added to the screening process. As a kind of overwintering crops, oilseed rape would grow after emergence until wintering period, and thus NDVI increases from October to December; the greenness or growth vigor would decline

at the yellow maturity stage relative to the peak growing season, and NDVI decreases accordingly from March to May. We created a mask to refine the extracted oilseed rape distribution in each growing season according to the change trends of NDVI described above, and the selection of data acquisition time was relatively flexible, good quality was the primary requirement. It should be noted that oilseed rape is usually transplanted among the lines of cotton in many places south of the Huaihe River, the cotton stalk will remain in the fields for a long time after harvest, during which it turns withered continuously, and the signal of oilseed rape will be overwhelmed at remote sensing scales due to its low biomass level. For this consideration, we did not take into account the trend of NDVI before wintering period for the vast area south of the Huaihe River.

3.3 Evaluation of freezing injury

3.3.1 Damage degree assessment

The MODIS daily surface reflectance data were used to calculate vegetation indices to indicate the freezing damage of oilseed rape. We first selected four widely used VIs to investigate their respective sensitivity to freezing injury (Table 1), and the MOD09GA data of 9 dates, i.e., January 13, 22, 24, 27, 31 and February 5, 9, 14, 27 from pre- to post-freeze were employed to produce the VIs. Taking into account the different numerical ranges of the selected VIs, we adopted the ratio relationship to examine each VI's behavior with time, namely the value of one specific VI at the beginning was set to '1' (as the baseline), and the subsequent values of the VI in the time series were set as the ratio of their initial values to that at the start.

Table 1 Vegetation indices selected for sensitivity analyses

Vegetation Index	Abbreviation	Expression	Reference
Normalized Difference Vegetation Index	NDVI	$(\rho_{NIR}-\rho_{Red})/(\rho_{NIR}+\rho_{Red})$	[23]
Enhanced Vegetation Index	EVI	$2.5\times(\rho_{NIR}-\rho_{Red})/(\rho_{NIR}+6\times\rho_{Red}-7.5\times\rho_{Blue}+1)$	[24, 25]
Green NDVI	GNDVI	$(\rho_{NIR}-\rho_{Green})/(\rho_{NIR}+\rho_{Green})$	[26]
Soil-Adjusted Vegetation Index	SAVI	$1.5\times(\rho_{NIR}-\rho_{Red})/(\rho_{NIR}+\rho_{Red}+1)$	[27]

Note: ρ_{Blue}, ρ_{Green}, ρ_{Red} and ρ_{NIR} denote the reflectance of blue, green, red and near infrared bands, respectively.

Empirically, it is generally assumed that there is a lag between the emergence of freezing weather and the corresponding vegetation responses. So the value of VI when crop responds adequately to freezing stress can be thought as the most representative of the actual impact of low temperature. To determine the freezing-induced VI departure from the normal state, the VI values in adjacent normal (freezing damage-free) growing seasons were used as the surrogate of the baseline. The detailed description of damage degree assessment is as follows:

1) During the period deemed as the freezing injury occurred, the minimum VI value was regarded as an indicator representing the influence of freezing process. However, multi-temporal data describing the freezing-affected crop growth were required in view of the missing values caused by cloud cover. For each pixel location, all the valid VI values from the dates when crop growth was obviously weakened were averaged according to the number of clear sky observations, and the result was recorded as VI_{2004}. We argue that maximum-composite approach is inappropriate for handling the multi-temporal VI data, for the consequent underestimation of damage severity.

2) The VI values of oilseed rape in 2001-2006 (excluding 2004) were calculated and taken as its normal growth level, given that the distribution of oilseed rape in each growing season was correctly filtered out. For a specific freezing damage-free growing season, the VI values of the same time frame as defined in step 1 were calculated and averaged according to clear sky numbers.

3) The annual VI values of the five growing seasons were averaged (result was recorded as VI_{base}) and the standard deviation was also calculated (recorded as δ). Taking into account the interannual fluctuations of crop growth, the difference between VI_{base} and δ, i.e., VI_{base}-δ, was taken as the floor growth level in a 'normal' growing season.

4) The degree of the freezing damage of oilseed rape in 2004 is then calculated as:

$$\frac{VI_{2004}-(VI_{base}-\delta)}{VI_{base}-\delta}\times 100\% \quad (1)$$

which was further used to mapping the distribution of

different freezing damage levels.

3.3.2 Supporting the results

Due to the lack of field observations, remote sensing-derived freezing damage intensity cannot be validated directly. As an alternative, the daily minimum temperature is believed as the most important damage-inducing factor of crop's freezing injury, in this section, we employed the correlation between the observed temperature and remote sensing-derived freezing damage degree to support the results. Moreover, low-temperature process usually lasts for several days, hence we chose its accumulated form so as to reveal the effect of low temperature duration.

Since oilseed rape can resist a certain degree of freeze with minimal impact, only the dates with minimum temperature less than –3°C (by reference to the observations from Hefei meteorological station), i.e., January 22-25, 27-28 and February 6-7, were selected in the following analyses. The statistical average damage degree of each major oilseed rape producing county was calculated, and the daily minimum temperature observed by the meteorological station of the corresponding county was also added up, a scatterplot was then generated to investigate their correlation.

3.4 Tracing the development of freezing injury

Five physiological indicators associated with vegetation biophysical or biochemical parameters were used to investigate the freezing response of oilseed rape over time, and they were derived from MODIS and MERIS Level 1 top-of-atmosphere radiance products. The acquisition dates were different due to the differences between the two sensors in revisit frequency and weather conditions during the overpass time.

MODIS-PRI, an indicator of light/radiation use efficiency (LUE/RUE), provides an effective measure of relative photosynthetic rates. It is defined as:

$$PRI = (\rho_{ref} - \rho_{531}) / (\rho_{ref} + \rho_{531}) \quad (2)$$

where, ρ_{531} is the reflectance at 531 nm, which is functionally related to the de-epoxidation state of the xanthophyll cycle; ρ_{ref} is the reflectance of the reference band, which is introduced in order to minimize the effects arising from sun angle variation[28]. For MODIS, bands 10, 12, 13 and 14 have been used as the reference band[14]. In this study, we selected bands 12 (546-556 nm) and 11 (526-536 nm) to generate PRI.

MODIS-NDWI (Normalized Difference Water Index), is intended to monitoring vegetation liquid water status[29]. In general, NDWI increases as the vegetation area fraction increases. The NDWI value for green vegetation is positive due to the weak liquid water absorption near 1.24 μm, and tends to be negative for most bare soils. NDWI is defined as:

$$NDWI = (\rho_{860} - \rho_{1240}) / (\rho_{860} + \rho_{1240}) \quad (3)$$

where, ρ_{860}, ρ_{1240} are the reflectance of wavelength at 860 nm and 1240 nm, corresponding to MODIS bands 2 and 5.

MERIS-REP (Red Edge Position), represents the region of abrupt change in leaf reflectance between 670 nm and 780 nm caused by the combined effects of strong chlorophyll absorption in the red wavelengths and high reflectance in the NIR[30]. REP is closely related with the growth and health status of vegetation, and has been used as a means to estimate foliar chlorophyll content[31,32] and LAI[33]. The shifts in the REP to shorter wavelengths can also serve as an indicator of vegetation stress[34]. We employed the linear interpolation method proposed by Guyot et al.[35] to estimate REP based on MERIS bands, which was more recently given in the work by Nguy-Robertson et al.[36] as:

$$R_i = \frac{\rho_{665} + \rho_{778.75}}{2} \quad (4)$$

$$REP = 708.75 + 45 \times \frac{R_i - \rho_{708.75}}{\rho_{753.75} - \rho_{708.75}} \quad (5)$$

where, ρ_{665}, $\rho_{708.75}$, $\rho_{753.75}$ and $\rho_{778.75}$ represent the reflectance of MERIS bands with the wavelength centered at 665 nm, 708.75 nm, 753.75 nm and 778.75 nm, or bands 7, 9, 10 and 12, respectively.

MERIS-MTCI (MERIS Terrestrial Chlorophyll Index), is more sensitive than REP to chlorophyll content, especially under the condition of high chlorophyll content[37]. MTCI is calculated as follows:

$$MTCI = (\rho_{753.75} - \rho_{708.75}) / (\rho_{708.75} - \rho_{681.25}) \quad (6)$$

where, $\rho_{681.25}$, $\rho_{708.75}$, $\rho_{753.75}$ are reflectance at the center wavelengths of the MERIS standard band setting, i.e., bands 8, 9 and 10, respectively.

MERIS-LAI was retrieved based on the TOA (top of atmosphere) algorithm[38], which couples atmosphere (SMAC), canopy (SAIL) and leaf (PROSPECT) radiative transfer models. TOA radiances in 13 MERIS bands other than the oxygen absorption (band 11) and water absorption (band 15) bands were used for the inversion. A BEAM-specific 'MERIS Vegetation Processors' plugin was applied to estimate LAI from MERIS Level-1P RR data (http://www.brockmann-consult.de/cms/web/beam/plug-ins?p_p_id=pluginsPortlet_WAR_beampluginsportlet10&version=4.11).

MODIS- and MERIS-NDVI were also used as a reference to demonstrate the different trends between the abovementioned indicators and the well-recognized NDVI. The MODIS red and NIR bands (1 and 2) were used for calculating NDVI, while MERIS-NDVI was derived from bands 7 and 12[16]. In addition, the Red Edge NDVI adopting MERIS band 9 (the red edge band) and band 12 as defined in [39] was also produced to compare the NDVIs generated with and without the red edge band in their responses to freezing injury.

4 Results

4.1 Oilseed rape growing regions

Taking the 2003–2004 growing season as example, Figure 4 shows the evolution of the general start time of bud and full-bloom stages in the whole province, and the extracted oilseed rape growing regions is also provided. The oilseed rape cultivated in different areas developed at different times, which could be screened out based on the identification of the key phenological phases through time-series analyses, and the union was regarded as its distribution in the study area. The oilseed rape fields in northern plains were sporadic, and the concentrated growing regions were distributed south of the Huaihe River, especially in Hefei and Chaohu in the Yangtze-Huaihe area, as well as the regions along the Yangtze River.

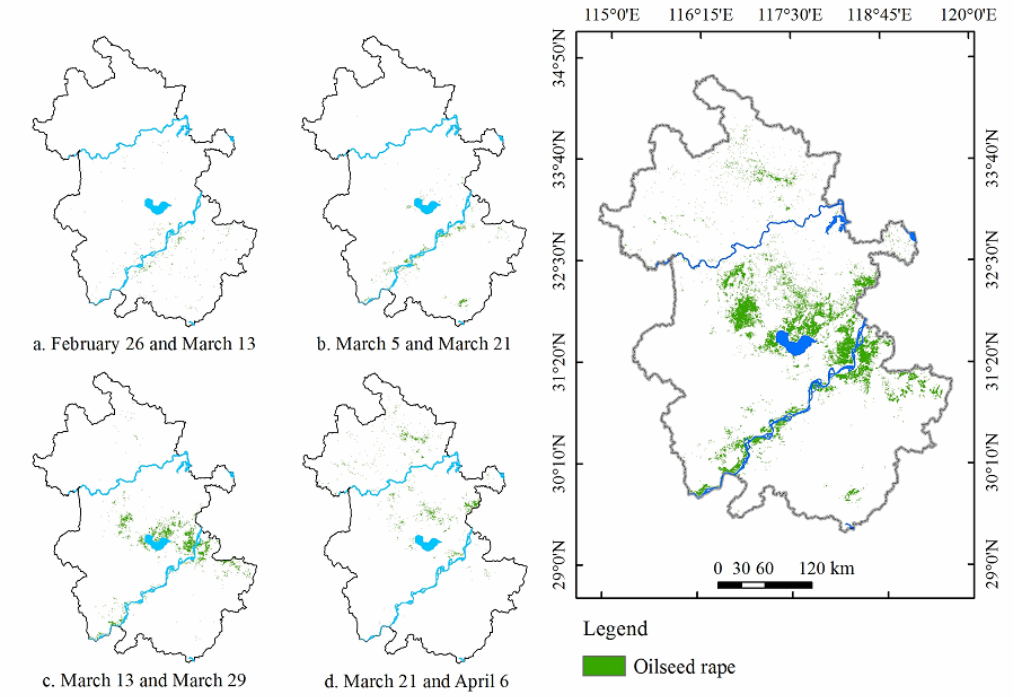

Figure 4 Evolution of crop phenology and the spatial distribution of oilseed rape in 2003-2004 growing season, labels a-d represent the start dates of bud stage and full-bloom stage

The resultant oilseed rape distributions in 2001-2006 were validated by means of the sown areas from statistical yearbooks, the acreage of oilseed rape for each municipal administrative unit was estimated and compared with statistics, and error was also evaluated and listed in Table 2.

The MODIS data applied to oilseed rape mapping is in coarse resolution (500 m), in consequence subtle ground features could not be captured. Obvious underestimation appeared generally in mountain dominated areas where the size of farmland was small in most cases, e.g., Lu'an, Anqing and Huangshan. By

contrast, overestimation arose in particular the regions where oilseed rape was concentrated, e.g., Chaohu and some of the areas along the Yangtze River, such as Ma'anshan. The poor accuracy in individual years 2002 and 2005 was attributed to the presence of abundant cloud in critical periods for oilseed rape identification. However, good results were achieved from the perspective of the whole province.

Table 2 Evaluation on the accuracy of oilseed rape extraction results

City	2001		2002		2003		2004		2005		2006	
	Extracted area/hm^2	Error/%	Extracted area/hm^2	Error/%	Extracted area/hm^2	Error/%	Extracted area/hm^2	Error/%	Extracted area/hm^2	Error/%	Extracted area/hm^2	Error/%
Hefei	158 625	21.3	180 325	32.25	171 775	23.89	100 775	–27.77	91 100	–36.11	57 625	–56.46
Huaibei	7750	–8.95	1450	–82.56	1800	–77.9	6250	–9.49	6425	31.07	3175	–22.26
Bozhou	12 725	–21.44	1450	–89.23	6375	–52.24	14 200	–4.06	17 200	55.85	7850	–16.47
Suzhou	35 650	–2.46	11 350	–71.15	31 475	–21.32	42 725	21.62	24175	–4.67	6650	–64.31
Bengbu	16 900	–10.12	20 425	–18.2	28 875	20.22	24 525	–1.32	8450	–59.09	3450	–74.02
Fuyang	8525	–47.71	275	–98.79	33 375	13.56	28 025	–16.64	3850	–87.67	33 175	19.66
Huainan	2525	41.22	675	–60.06	4250	88.14	5075	–18.03	5625	27.93	3025	–39.90
Chuzhou	102 375	–21.49	92 000	–27.39	185 925	40.54	84 700	–37.52	106 425	–12.21	39 725	–55.68
Lu'an	35 775	–73.28	155 500	–6.57	122 800	–25.93	85 100	–42.73	117025	–21.68	143 625	14.63
Ma'anshan	33 225	1.62	14 300	–56.85	49 050	46.56	29 850	–12.04	46 825	37.66	42 300	31.62
Chaohu	94 525	–25.85	86 275	–32.39	185 250	44.3	162 350	29.40	141 475	14.30	136 950	21.26
Wuhu	40 775	–8.65	11 775	–73.45	41 175	–5.76	43 875	0.21	47 100	8.33	42 250	5.08
Xuancheng	37 625	–52.47	70 300	–13.95	76 375	–6.25	45 800	–45.06	103 800	37.19	41 325	–32.51
Tongling	7225	–17.12	8300	–6.59	11 100	26.92	10 375	14.68	5750	–33.09	8925	5.61
Chizhou	27 075	–29.13	1500	–95.92	21 550	–38.91	25 875	–21.93	5000	–84.45	19 925	–33.92
Anqing	96 900	–5.53	8825	–91.56	66 075	–37	76 900	–27.41	21 250	–79.04	96 400	–5.26
Huangshan	15 475	–40.4	7200	–71.58	9625	–61	12 275	–47.76	6150	–74.14	17 425	–25.08
Total	733 675	–22.99	671 925	–32.96	1 046 850	3.19	801 475	–20.12	757 625	–20.55	703 800	–15.77

4.2 Freezing damage assessment

4.2.1 Freezing damage mapping

The temporal profiles of the selected four VIs are presented in Figure 5. The obvious troughs around February show that the oilseed rape was certainly affected by the freezing processes. SAVI and EVI responded similarly to the freezing stress, however, unexpected trajectories appeared in the segment between January 22 and 27. In addition, SAVI and EVI did not properly respond to the second freezing process occurred in early February. The trajectories of NDVI and GNDVI are more in accordance with the reality: the two freezing processes were properly reflected in the time series and the former was more serious than the latter one. It shows that NDVI outperforms GNDVI in terms of the sensitivity level, so it is selected as the freezing-injury indicator in the following analysis.

Figure 5 shows that, the NDVI trajectory has two minimum values on February 5 and 14, respectively. For one specific pixel (identified as oilseed rape) in the study area, the average NDVI values during this period in 2001-2006 were calculated. The degree of freezing damage is then represented by the departure of damage-affected NDVI from the benchmark level in February 5-14, as calculated by Equation (1). The negative value indicates that the oilseed rape has suffered freezing injury, as shown in Figure 6.

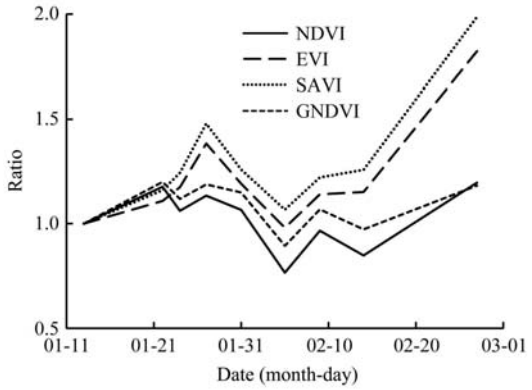

Figure 5 Temporal profiles of the selected VIs for the oilseed rape growing in the Yangtze-Huaihe area. Note that the value of each VI at the beginning of the time series is set to '1', and each time series is the average of 500 different ones

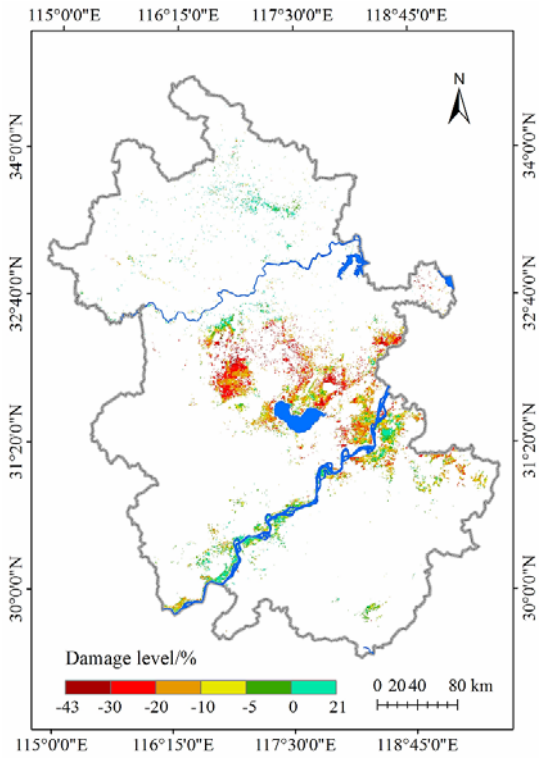

Figure 6 Spatial distribution (500 m gridded) of freezing damage levels

It shows that the oilseed rape cultivated in the Yangtze-Huaihe area was apparently injured, especially in the regions with relatively higher latitude. The regions along the Yangtze River were less affected, which could be attributed to the joint effect of the lower latitude and the relatively warm micro-climate brought about by the large water body of the Yangtze River. The southwestern part of the study area was least affected.

It should be noted that the oilseed rape growing in the northern plains and the areas near the Huaihe River was rarely affected by the freezing processes. This could be explained by the strong winterness varieties, mix-planting with wheat, and the coarse resolution of MODIS sensor.

4.2.2 Results support

The correlation between freezing damage degree and meteorological temperature was investigated to support the monitoring results. The oilseed rape cultivated in northern plain has greater cold resistance, which is less affected by freezing weather. No apparent damage was observed in this area from Figure 6, therefore we did not take the counties north of the Huaihe River into consideration.

Total 48 major oilseed rape producing counties in the study area were selected, the statistical average damage degree and the accumulated daily minimum temperature during freezing processes for each county were calculated as described previously, and then a scatterplot was generated. A significant correlation between these two variables was observed (Figure 7), which justified the remote sensing-derived damage map in a manner.

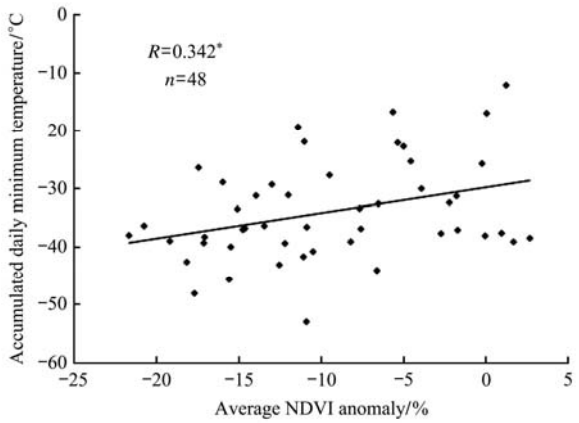

Note: * indicates significance at the 0.05 level.

Figure 7 Correlation between the statistical average of remote sensing-derived damage degree and the accumulated temperature involving 48 oilseed rape producing counties

4.3 Characterizing damage development

The time series of physiological indicators were generated by means of stratified random sampling points selected from the oilseed rape fields in the study area. Total 206 and 104 sampling points were selected at the MODIS- and MERIS-pixel scales, respectively. For each indicator, we took the average of the time series extracted by the sampling points as the representative temporal profile of the specific indicator.

4.3.1 Performance of MODIS-PRI and NDWI

The temporal profiles of PRI and NDWI both derived from MODIS bands are shown in Figures 8 and 9 (the time series of NDVI is used as a reference). It should be noted that the MODIS L1B data acquired on January 27, 2004 appeared much hazier than the surface reflectance product (MOD09GA), so we discarded this granule.

PRI decreased dramatically after the attack of cold wave, and the amplitude of variation is greater than NDVI (76.8% vs. 53.7%). Moreover, the magnitude of PRI was still obviously lower than NDVI during the recovery phase, indicating that the photosynthetic rate of oilseed rape was highly sensitive to freezing stress.

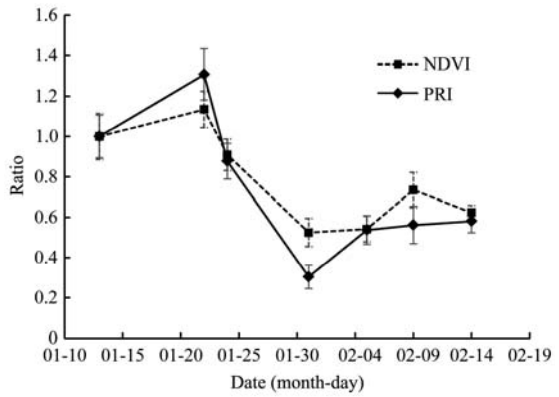

Figure 8 Temporal profiles of MODIS-PRI and NDVI. The value of each VI at the beginning is set to '1'; the data of PRI on February 27 is missing due to the imaging quality problems of MODIS band 12

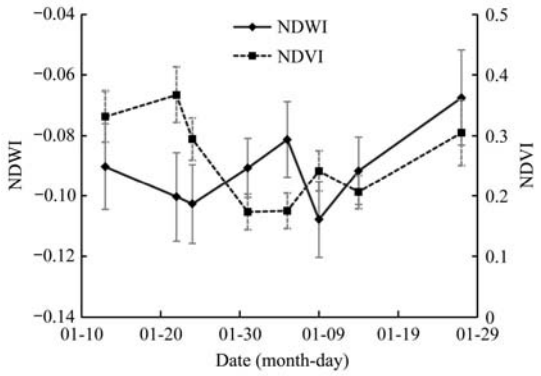

a

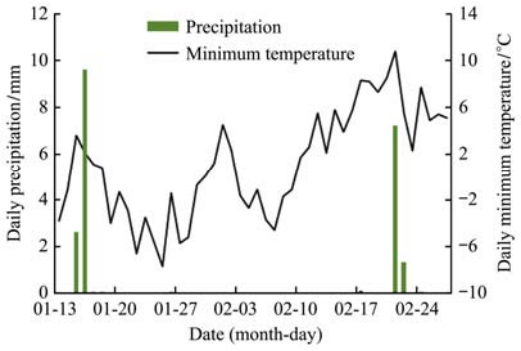

b

Figure 9 Temporal profiles of MODIS-NDWI and NDVI (a), and daily precipitation (observed in Hefei) from January 13 to February 27, 2004 (b)

The temporal sequence of NDWI is given in Figure 9a, in which the NDVI is also introduced for ease of comparative analysis. There was little precipitation during this period (Figure 9b), therefore the impact of rainfall on vegetation water content could roughly be ruled out, and the sudden changes of canopy water status could be mostly attributed to freezing injury. All the NDWI values are negative, indicating that the aboveground biomass was at low levels and the soil background was evident in wintertime. In general, the two VIs trend in opposite ways most of the time, and the increased NDWI values when oilseed rape was obviously injured indicate the occurrence of foliage water loss (during the overpass of Terra-MODIS in the morning). NDWI increases along with NDVI later in the recovery and regrowth stage (after February 14), indicating that the impact of freezing injury has ended.

4.3.2 Performance of MERIS-LAI

Figure 10 demonstrates the trajectories of LAI and NDVI derived from MERIS data. The minimal values in NDVI temporal profile reveal the influence of freezing weather occurred in late January and early February. A slow response of LAI was observed, indicating its lower sensitivity to freezing injury compared with NDVI. LAI did not drop immediately with the advent of freezing process; additionally, it restored quickly after the impact of freezing stress.

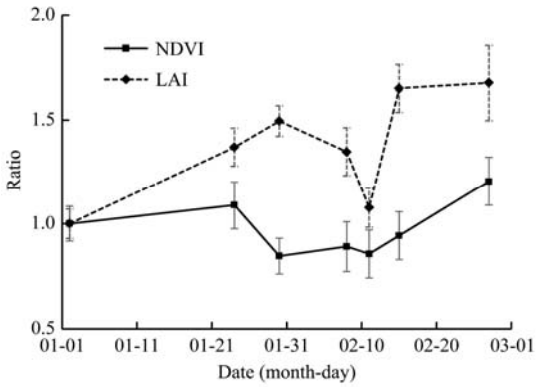

Figure 10 Temporal profiles of LAI and NDVI derived from MERIS data, the value of each at the beginning is set to '1'

4.3.3 Performance of MERIS-MTCI and REP

MERIS-MTCI and REP show the trends of monotonic increase, in spite of the freezing injury events (Figure 11). Since MTCI is well known to be an effective indicator of chlorophyll content, it is deduced that the canopy chlorophyll content was not reduced by the freezing damage. However, the increase in MTCI value was suppressed by freezing stress to a certain degree (the segment between January 3 and February 8 as shown in Figure 11a). REP was generally not affected by freezing injury (Figure 11b), its insensitivity could also be demonstrated by the time series of red edge NDVI. With the adoption of the red edge band (band 9), MERIS-NDVI showed an apparently reduced sensitivity

to freezing injury (Figure 12).

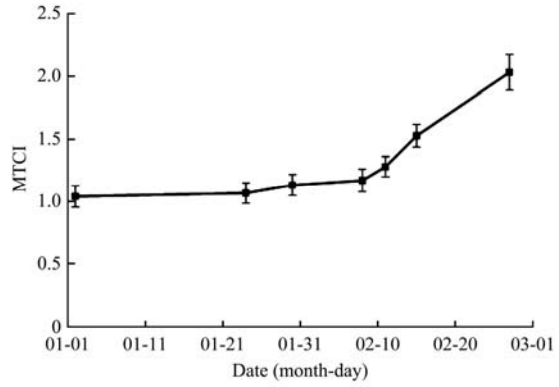

a

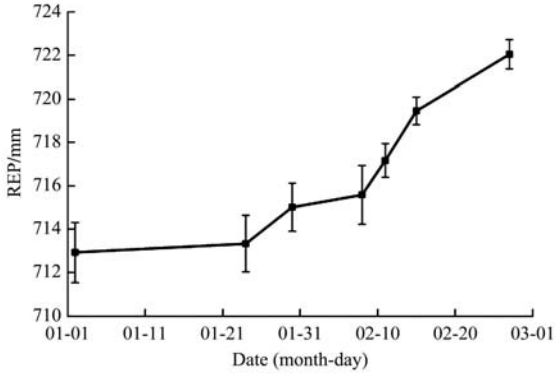

b

Figure 11 Temporal profiles of MERIS-MTCI (a) and REP (b)

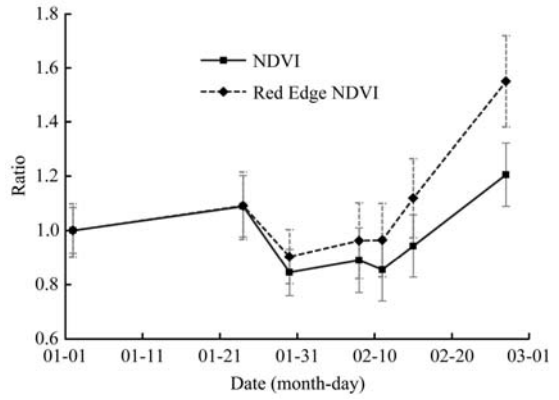

Figure 12 Temporal profiles of MERIS-NDVI (produced adopting bands 7 and 12) and red edge NDVI (adopting bands 9 and 12). The value of each VI at the start date is set to '1'.

5 Discussion

In this paper, we mapped the distributions of oilseed rape in 2001-2006, evaluated the severity of its freezing injury occurred in 2004, and investigated the temporal patterns of specific crop physiological indicators under freezing stress based on MODIS and MERIS data. We found that NDVI and plant photosynthesis-associated VI, i.e., PRI was more sensitive to freezing stress.

The method of crop phenology identification requires time-series NDVI data, and the result depends largely on data quality. The seasonal shifts play an important role on the availability of remote sensing data, the activity of cold air is especially frequent in late autumn and early spring, which falls within the time frame covered by this study, there will be more cloud amount in the sky and clear observations are reduced to a great extent. The empty values arising from cloud cover cannot be effectively reconstructed through S-G filtering procedure, which largely explains the poor accuracy of oilseed rape acreage in 2001-2002 and 2004-2005 growing seasons since long-term cloudy weather appeared in key pheonological phases. In addition, the administrative boundary of many counties changed in history, the vector boundary used in this paper may not be in line with the actual situation of that period, leading to unexpected errors in the validation step.

NDVI and EVI respond differently to freezing stress, and we show that NDVI performs better in freezing injury detection than EVI at MODIS-pixel scale, though the latter is usually considered to be less sensitive to soil background noise, and not easily to saturate[40]. Huete et al.[25] argued that NDVI was more sensitive to canopy parameters associated with the absorbed photosynthetically active radiation, whereas EVI was more sensitive to structural canopy parameters such as LAI, biomass, and leaf morphology. Since photosynthesis is proven to be highly sensitive to low-temperature stress from the present study, the better performance of NDVI over other commonly used VIs, e.g., EVI, SAVI and GNDVI in freezing injury detection could be partially explained by its coupling with photosynthetic efficiency. In addition, Wardlow et al.[41] found that NDVI had greater sensitivity across low to intermediate green biomass levels compared with EVI, which might help capture more subtle variations among crops during the early growing stage. During the wintering period, the oilseed rape is still in seedling stage and the aboveground biomass is low. In this regard, the well-performed NDVI in freezing damage monitoring makes sense, moreover, there is definitely no saturation problem.

Low temperature is the foremost damage-inducing

factor for freezing damage, the gridded daily minimum temperature data is therefore urgently demanded in the assessment of freezing injury. However, LST derived from thermal infrared band(s) is actually unpractical due to the availability of data, freezing weather is usually accompanied by dense cloud cover in southern China—the main producing area of winter oilseed rape. Furthermore, a low-temperature process usually lasts for only a couple of days, so the qualified remote sensing images are hard to guarantee. Future study will consider other technical means to identify freezing injury timely and more efficiently, e.g., by downscaling microwave brightness temperature.

Freezing injury impacts various biophysical and biochemical parameters of oilseed rape in different ways. The time series of certain physiologically related indicators could reveal their respective sensitivity to freezing injury, and provide a brief description of the change patterns of the corresponding physiological parameters under freezing stress. The present study shows the performance of the investigated indicators in their responses to freezing injury, and the well-behaved VIs are thereby appreciated. The findings are proposed based on the work carried out solely at remote sensing level, however, the significance of our research lies in that it provides a theoretical basis for remote sensing monitoring of freezing injury from the perspective of physiological variables. We look forward to developing special index for the rapid identification of freezing damage, the relevant MODIS bands responding to photosynthesis and canopy water status could be used for reference.

Further study will also focus on validating the relationship between remote sensing indicators and crop physiological parameters, by means of field observations using dedicated instruments. The big challenges are the diverse terrain and climatic conditions within the study area, therefore we have to set up adequate and representative sampling sites, which brings a huge workload. In addition, the fragmented croplands make it more difficult to match between remote sensing-derived results and filed-measured data in view of the coarse footprint of MODIS or MERIS pixels.

Uncertainties might exist due to the ‘mixed-pixel’ effect caused by the coarse resolution of remote sensors, as well as the heterogeneous and fragmented ground surface in the study area, especially in the Yangtze-Huaihe area. The weak crop signals, frequent cloud cover, as well as the strong soil background noise in wintertime all interfere with freezing injury assessment by remote sensing.

6 Conclusions

The high revisit frequency along with the abundant band set for medium resolution imaging spectrometers guarantee effective assessment of oilseed rape freezing injury and revealing the damage development characteristics at medium to large scales. In this study, we achieved the abovementioned objectives by using the data acquired from MODIS and MERIS sensors, regardless of the unfavorable factors in the early growing stages, e.g., weak crop signals and strong background noise.

Time series analysis has advantages in crop phenology identification, we can screen out oilseed rape based on the reduction of its greenness in full-bloom period relative to bud stage. The Normalized Differenced Vegetation Index (NDVI) is more sensitive to freezing injury compared with the other commonly used vegetation indices, i.e., EVI, GNDVI and SAVI, and it is qualified to be the freezing damage indicator at MODIS-pixel scale. The time frame when oilseed rape responds adequately to freezing injury is critical to determining the damage intensity. The relatively weak winterness of the oilseed rape growing in the Yangtze-Huaihe area makes it more susceptible to freezing injury, and the actual damage extent depends on the geographic position, as well as the micro climate brought about by large water body, e.g., the Yangtze River.

The photosynthesis of oilseed rape is very sensitive to freezing injury, which could be demonstrated by the temporal profile of PRI (Photochemical Reflectance Index, indicator of photosynthetic rate). The better performance of NDVI over other tested VIs in terms of damage response is speculated to be attributed to its

association with photosynthetic variables. Whereas the slow and lagging response of MERIS leaf area index (LAI) to freezing injury reveals its low sensitivity. Freezing injury causes the abnormal increase of canopy water content (represented by NDWI), indicating the occurrence of canopy water loss after the attack of cold wave. There is no evidence that the canopy chlorophyll content is reduced by freezing stress from the present research, deducing from the behavior of REP (Red Edge Position) and MTCI (MERIS terrestrial chlorophyll index), in the context of mild to moderate damage degree. It appears that freezing injury impacts the physiological functions (e.g., photosynthesis) the most, followed by canopy structure (e.g., green leaf area), and the organic content (e.g., canopy chlorophyll content) of the oilseed rape.

The findings proposed in this study are of significance in the practice of remote sensing monitoring of oilseed rape freezing injury in southern China.

Acknowledgements

This research was funded by the National Natural Science Foundation of China (No. 41171276). We are grateful to Song Xiaodong (Zhejiang University, China) for his comments and suggestions, which greatly help improve this manuscript. We would also like to express our sincere thanks to the anonymous reviewers for their constructive comments.

[References]

[1] Cannell M G R, Smith R I. Climatic warming, spring budburst and forest damage on trees. J. Appl. Ecol, 1986; 23(1): 177–191.

[2] Gu L H, Hanson P J, Mac Post W, Kaiser D P, Yang B, Nemani R, et al. The 2007 Eastern US spring freeze: Increased cold damage in a warming world? BioScience, 2008; 58(3): 253–262.

[3] Lardon A, Triboi-Blondel A M. Freezing injury to ovules, pollen and seeds in winter rape. J. Exp. Bot, 1994; 45(277): 1177–1181.

[4] Rapacz M. Cold-deacclimation of oilseed rape (*Brassica napus* var. *oleifera*) in response to fluctuating temperatures and photoperiod. Ann. Bot, 2002; 89(5): 543–549.

[5] Lardon A, Triboi-Blondel A M. Cold and freeze stress at flowering Effects on seed yields in winter rapeseed. Field Crop. Res, 1995; 44(2): 95–101.

[6] Behrens T, Diepenbrock W. Using digital image analysis to describe canopies of winter oilseed rape (*Brassica napus* L.) during vegetative developmental stages. J. Agronomy & Crop Science, 2006; 192(4): 295–302.

[7] Silleos N, Perakis K, Petsanis G. Assessment of crop damage using space remote sensing and GIS. Int. J. Remote Sens, 2002; 23(3): 417–427.

[8] Wang H F, Gu X H, Wang J H, Dong Y Y. Monitoring winter wheat freeze injury based on multi-temporal data. Intell. Autom. Soft Comput, 2012; 18(8): 1035–1042.

[9] Jurgens C. The modified normalized difference vegetation index (mNDVI) a new index to determine frost damages in agriculture based on Landsat TM data. Int. J. Remote Sens, 1997; 18(7): 3583–3594.

[10] Feng M C, Yang W D, Cao L L, Ding G W. Monitoring winter wheat freeze injury using multi-temporal MODIS data. Agric. Sci. China, 2009; 8(9): 1053–1062.

[11] Currit N, St Clair S B. Assessing the impact of extreme climatic events on aspen defoliation using MODIS imagery. Geocarto Int, 2010; 25(2): 133–147.

[12] Tan Z, Ding M, Yang X, Ou Z. Monitoring freeze injury and evaluating losing to sugar-cane using RS and GPS. International Conference on Computer and Computing Technologies in Agriculture. Springer: Boston, US, 2009; 293: 307–316.

[13] Kerdiles H, Grondona M, Rodriguez R, Seguin B. Frost mapping using NOAA AVHRR data in the Pampean region, Argentina. Agric. For. Meteorol, 1996; 79(3): 157–182.

[14] Garbulsky M F, Peñuelas J, Gamon J, Inoue Y, Filella I. The photochemical reflectance index (PRI) and the remote sensing of leaf, canopy and ecosystem radiation use efficiencies: A review and meta-analysis. Remote Sens. Environ, 2011; 115(2): 281–297.

[15] Chandrasekar K, Sesha Sai M V R, Roy P S, Dwevedi R S. Land Surface Water Index (LSWI) response to rainfall and NDVI using the MODIS Vegetation Index product. Int. J. Remote Sens, 2010; 31(15): 3987–4005.

[16] Van Der Meer F, Bakker W, Scholte K, Skidmore A, De Jong S, Clevers J, et al. Spatial scale variations in vegetation indices and above-ground biomass estimates: Implications for MERIS. Int. J. Remote Sens, 2001; 22(17): 3381–3396.

[17] Xiong X, Sun J, Wu A, Chiang K F, Esposito J, Barnes W. Terra and Aqua MODIS calibration algorithms and uncertainty analysis. Remote Sensing. International Society for Optics and Photonics, Bruges, Belgium, October 21, 2005; pp. 59780V–59780V-10.

[18] Xiao X M, Boles S, Liu J Y, Zhuang D F, Frolking S, Li C S, et al. Mapping paddy rice agriculture in southern China

using multi-temporal MODIS images. Remote Sens. Environ, 2005; 95(4): 480–492.

[19] Xiao X M, Boles S, Frolking S, Li C S, Babu J Y, Salas W, et al. Mapping paddy rice agriculture in South and Southeast Asia using multi-temporal MODIS images. Remote Sens. Environ, 2006; 100(1): 95–113.

[20] Chen J, Jönsson P, Tamura M, Gu Z, Matsushita B, Eklundh L. A simple method for reconstructing a high-quality NDVI time-series data set based on the Savitzky–Golay filter. Remote Sens. Environ, 2004; 91(3): 332–344.

[21] Ren J, Chen Z, Zhou Q, Tang H. Regional yield estimation for winter wheat with MODIS-NDVI data in Shandong, China. Int. J. Appl. Earth Obs. Geoinf, 2008; 10(4): 403–413.

[22] Jönsson P, Eklundh L. TIMESAT—a program for analyzing time-series of satellite sensor data. Comput. Geosci, 2004; 30(8): 833–845.

[23] Rouse J W, Haas R H, Schell J A, Deering D W, Harlan J C. Monitoring the vernal advancements and retrogradation of natural vegetation. NASA/GSFC, Final Report, Greenbelt, MD, USA, 1974; pp. 1–137.

[24] Liu H Q, Huete A R. A feedback based modification of the NDVI to minimize canopy background and atmospheric noise. IEEE Trans. Geosci. Remote Sens, 1995; 33(2): 457–465.

[25] Huete A R, Liu H Q, Batchily K, van Leeuwen W. A comparison of vegetation indices over a global set of TM images for EOS-MODIS. Remote Sens. Environ, 1997; 59(3): 440–451.

[26] Gitelson A A, Kaufman Y J, Merzlyak M N. Use of a green channel in remote sensing of global vegetation from EOS-MODIS. Remote Sens. Environ, 1996; 58(3): 289–298.

[27] Huete A R. A soil-adjusted vegetation index (SAVI). Remote Sens. Environ, 1988; 25(3): 295–309.

[28] Gamon J A, Peñuelas J, Field C B. A narrow-waveband spectral index that tracks diurnal changes in photosynthetic efficiency. Remote Sens. Environ, 1992; 41(1): 35–44.

[29] Gao B C. NDWI—a normalized difference water index for remote sensing of vegetation liquid water from space. Remote Sens. Environ, 1996; 58(3): 257–266.

[30] Horler D N H, Dockray M, Barber J. The red edge of plant leaf reflectance. Int. J. Remote Sens, 1983; 4(2): 273–288.

[31] Curran P J, Dungan J L, Macler B A, Plummer S E. The effect of a red leaf pigment on the relationship between red edge and chlorophyll concentration. Remote Sens. Environ, 1991; 35(1): 69–76.

[32] Blackburn G A. Remote sensing of forest pigments using airborne imaging spectrometer and LIDAR imagery. Remote Sens. Environ, 2002; 82(2): 311–321.

[33] Pu R, Gong P, Biging G S, Larrieu M R. Extraction of red edge optical parameters from Hyperion data for estimation of forest leaf area index. IEEE Trans. Geosci. Remote Sens, 2003; 41(4): 916–921.

[34] Smith K L, Steven M D, Colls J J. Use of hyperspectral derivative ratios in the red-edge region to identify plant stress responses to gas leaks. Remote Sens. Environ, 2004; 92(2): 207–217.

[35] Guyot G, Baret F, Jacquemoud S. Imaging spectroscopy for vegetation studies. Imaging spectroscopy: Fundamentals and prospective application, 1992; 2: 145–165.

[36] Nguy-Robertson A L, Peng Y, Gitelson A A, Arkebauer T J, Pimstein A, Herrmann I, et al. Estimating green LAI in four crops: Potential of determining optimal spectral bands for a universal algorithm. Agric. For. Meteorol, 2014; 192: 140–148.

[37] Dash J, Curran P J. The MERIS terrestrial chlorophyll index. Int. J. Remote Sens, 2004; 25(23): 5403–5413.

[38] Baret F, Pavageau K, Beal D, Weiss M, Berthelot B, Regner P. Report on the algorithm theoretical basis document for MERIS Top of Atmosphere Land Products (TOA_VEG). Contract ESA AO/1-4233/02/I-LG, 2006.

[39] Gitelson A A, Merzlyak M N. Spectral reflectance changes associated with autumn senescence of *Aesculus hippocastanum* L. and *Acer platanoides* L. leaves. Spectral features and relation to chlorophyll estimation. J. Plant Physiol, 1994; 143(3): 286–292.

[40] Gao X, Huete A R, Ni W G, Miura T. Optical–biophysical relationships of vegetation spectra without background contamination. Remote Sens. Environ, 2000; 74(3): 609–620.

[41] Wardlow B D, Egbert S L, Kastens J H. Analysis of time-series MODIS 250 m vegetation index data for crop classification in the US Central Great Plains. Remote Sens. Environ, 2007; 108(3): 290–310.